Atmospheric Disturbances Caused by Human Modification of the Landscape

Christopher P. Weaver and Roni Avissar
Center for Environmental Prediction, Rutgers–The State University of New Jersey,
New Brunswick, New Jersey

ABSTRACT

This study documents significant atmospheric effects over the U.S. central plains caused by human modification of the landscape. Using observations and an atmospheric model, it is shown here that diurnal, thermally induced circulations occur during summer over a 250 × 250 km region in Oklahoma and Kansas. Furthermore, it is shown that the driving force behind these circulations is the landscape heterogeneity resulting from differential land use patterns, that such atmospheric phenomena are characteristic of surfaces with this type of heterogeneity and not limited to infrequent days when unusual wind or other meteorological conditions prevail, and that the net effect of these motions is significant, not only locally, but also at the regional and global scales.

1. Introduction

Parallel questions currently face those who study climate and climate change: in what ways are humans impacting the climate system, and do scientists and policy makers have the ability to predict future change resulting from this impact? One of the areas in which our understanding of both questions is most limited is that of the effect, on atmospheric processes, of human-induced changes of the landscape.

Variability in land properties occurs at a continuum of spatial scales. As deforestation, shifts in agriculture, and urbanization rise dramatically, natural vegetation patterns are modified, resulting in a complex and heterogeneous patchwork of surface characteristics unique to a given region. The interaction between these landscapes and the overlying atmosphere has a powerful effect on the way heat, moisture, momentum, dust, and pollutants move upward from the surface into the atmosphere.

The fluxes of heat and moisture from the surface into the adjacent atmosphere are fundamental driving forces of atmospheric motions in the planetary boundary layer (PBL; Stull 1988), and the response of the atmosphere to this forcing depends strongly on the scale of the landscape variability that determines the distribution of these fluxes. For a domain characterized by horizontal variability in surface sensible heat (SH) and latent heat (LH) fluxes, theory suggests that there are two different atmospheric responses, depending on the scale of the variability (Vidale et al. 1997; Baidya Roy and Avissar 2000; Avissar and Schmidt 1998; Dalu et al. 1996; Chen and Avissar 1994a; Wang et al. 1998). For landscape heterogeneity with typical scales on the order of 5 km or less (such a land surface pattern might therefore "look" homogeneous at much larger scales), the atmospheric response consists solely of chaotic motions (turbulence) with eddies that have a scale on the order of the PBL depth. For patterns that consist of areas of similar surface fluxes covering distances greater than this, with individual patches up to about 100–200 km, it is suggested that the randomly distributed turbulent motions can organize into much larger systems, commonly referred to as mesoscale circulations, oriented according to the

Corresponding author address: Christopher P. Weaver, Center for Environmental Prediction, Department of Environmental Sciences, Rutgers–The State University of New Jersey, 14 College Farm Road, New Brunswick, NJ 08901-8551.
E-mail: weaver@cep.rutgers.edu.
In final form 6 October 2000.
©2001 American Meteorological Society

underlying landscape heterogeneity and at a similar spatial scale. Observations of the scope necessary to validate these ideas are sparse, but a few studies have identified possible signatures of landscape-induced mesoscale circulations in certain regions and for certain conditions (Rabin et al. 1990; Bougeault et al. 1991; Cutrim et al. 1995; Brown and Arnold 1998). Other observational studies, focusing on regions where such effects might be expected, have either found no evidence for them or found that any resulting circulations are very weak (Mahrt et al. 1994; Doran et al. 1995; Hubbe et al. 1997). Various investigations using numerical models have suggested that these circulations can be intense, may play an influential role in producing and organizing clouds and precipitation, and could have effects that are significant at scales much larger than simply the scale of the systems themselves (Pielke et al. 1991; Segal et al. 1988; Segal et al. 1989; Ookouchi et al. 1984; Mahfouf et al. 1987; Yan and Anthes 1988; Avissar and Pielke 1989; Pinty et al. 1989; Chen and Avissar 1994b; Lynn et al. 1995b; Seth and Giorgi 1996; Avissar and Liu 1996). These earlier model studies have tended to report on the results from highly idealized simulations, thus making it difficult to assess their relevance for insights into real-world processes. More recent work, however, has moved in the direction of better observational constraint of surface characteristics, the incorporation of realistic, synoptic-scale meteorology into the numerical integrations, and the use of more complex modeling systems run at higher spatial resolutions (Vidale et al. 1997; Zhong and Doran 1997, 1998). These more recent and realistic treatments of the problem have only sharpened the debate regarding the importance of mesoscale landscape effects in the context of climate and climate prediction. We use a mesoscale numerical model in conjunction with observations to investigate the impact of landscape heterogeneity on atmospheric processes over the central United States. The results documented here provide a clear demonstration that landscape heterogeneities produce mesoscale atmospheric effects of a scope and significance that is not limited to small areas and rare conditions.

2. Methods and data

Our basic methodology is to perform simulations using a mesoscale model, namely, the Colorado State University Regional Atmospheric Modeling System (RAMS; Pielke et al. 1992; Liston and Pielke 2000), of several case-study days observed at the Department of Energy Atmospheric Radiation Measurement (ARM) Cloud and Radiation Testbed (CART) in Oklahoma and Kansas (Stokes and Schwartz 1994) as part of the Global Water and Energy Cycle Experiment (GEWEX) Continental Scale International Project (GCIP) Enhanced Seasonal Observing Period for 1995 (ESOP-95; Coughlan and Avissar 1996). Because of a lack of suitable observations of the complete atmospheric effects of mesoscale landscape heterogeneity, the only reasonable tool for a comprehensive investigation of this phenomenon is a numerical model.

The RAMS solves the full, nonlinear equations of motion for the atmosphere, and it includes parameterizations for turbulent fluxes, radiation, convection, and cloud microphysics, as well as a comprehensive soil and vegetation model. For this study, we take advantage of the nested (telescoping) grid capability of RAMS. We use three such nested grids centered on the CART site, with the innermost (Grid 3) covering 252 $\times$ 252 km with a horizontal grid spacing of 2 km, the next coarser grid (Grid 2) covering 720 $\times$ 720 km with a grid spacing of 8 km, and the coarsest grid (Grid 1) encompassing an area 1600 $\times$ 1600 km with a grid spacing of 32 km (Fig. 1a). This nesting of fine grids within coarse ones is a compromise, forced by existing limitations on computing technology, between simulating the region of interest with a high enough resolution to capture the important scales and processes and simulating a large enough domain to correctly represent all the relevant meteorological forcing. While we use the convective parameterization on Grid 1, we leave it turned off on Grids 2 and 3: particularly for 2-km grid spacing, use of the convective scheme would be inappropriate, and any convection occurring on the fine grids must therefore be explicitly resolved. There are 38 vertical levels from the surface to approximately 22 km, with half of these located in the first 3 km. The horizontal area of Grid 3 is comparable to that of a typical Global Climate Model (GCM) grid element, and thus we expect averages over this domain to represent the effects that a GCM should be required to simulate with reasonable fidelity.

We selected six case-study days to simulate: 6, 7, 10, 12, 13, and 21 July 1995. These particular days in July were chosen because the CART site was relatively unobscured by any extensive cloud systems of obvious large-scale (nonlocal) origin, thus making possible the identification of any signature of the local land surface. By this choice we do not mean to imply that landscape-induced mesoscale effects would necessarily be small on days when larger-scale cloud systems are present over the ARM/CART, simply that their possible effect on clouds and precipitation would be masked. Further simulations (not shown here) based on observations from other days when overall conditions were much more disturbed still produced strong mesoscale circulations.

The ARM/CART covers approximately 300 × 350 km in Oklahoma and Kansas, and this heavily instrumented site provides frequent measurements of surface SH and LH fluxes, as well as other surface properties, meteorology, and hydrology, at numerous stations within the domain and throughout the year (Stokes and Schwartz 1994). The human footprint on this region is readily apparent. During summer, large differences in land use across this site, particularly the contrast between winter wheat in the central portion of the domain, which is already harvested by July, and other crops and natural vegetation that are still actively growing elsewhere, contribute to significant gradients in surface fluxes (Hubbe et al. 1997; Zhong and Doran 1997, 1998; Doran et al. 1998). Taking advantage of the multiple observations of surface fluxes and meteorology, we use a gridded surface SH and LH flux dataset as the surface boundary condition for our RAMS simulations. This dataset is described in Doran et al. (1998) and was created by calculating fluxes, at a horizontal grid spacing of 6.25 × 6.25 km, using the Simple Biosphere Model (Sellers et al. 1996) forced with observed soil, vegetation, and meteorology. The resultant fluxes were then validated against observations from the ARM/CART flux measurement stations (taken every 30 min each day). This observationally derived flux dataset is specified as the surface boundary condition everywhere on the RAMS Grid 3, and for the portion of Grid 2 that covers the CART domain. For the remainder of Grid 2, and for Grid 1, the surface fluxes are calculated using the RAMS soil and vegetation model. A similar technique was used in Zhong and Doran (1998). Figure 1b shows early afternoon SH flux on Grid 3 for the 13 July case day. Flux contrasts on the order of 200 W m^{-2} are apparent between areas (patches) with characteristic scales of 20–100 km. The relative roles of evaporation from moist or vegetated surfaces and direct heating of dry surfaces lead to compensation between surface SH and LH flux. As a result, the LH flux field for this domain exhibits a pattern that is essentially the inverse of the SH flux shown in Fig. 1b, with similar magnitude. The pattern of surface fluxes on all days is similar, though not identical, to the 13 July case shown in Fig. 1b and evolves slowly throughout the month (Zhong and Doran 1998). This relative steadiness in surface fluxes over time underscores the fact that it is the differen-

(a) (b)

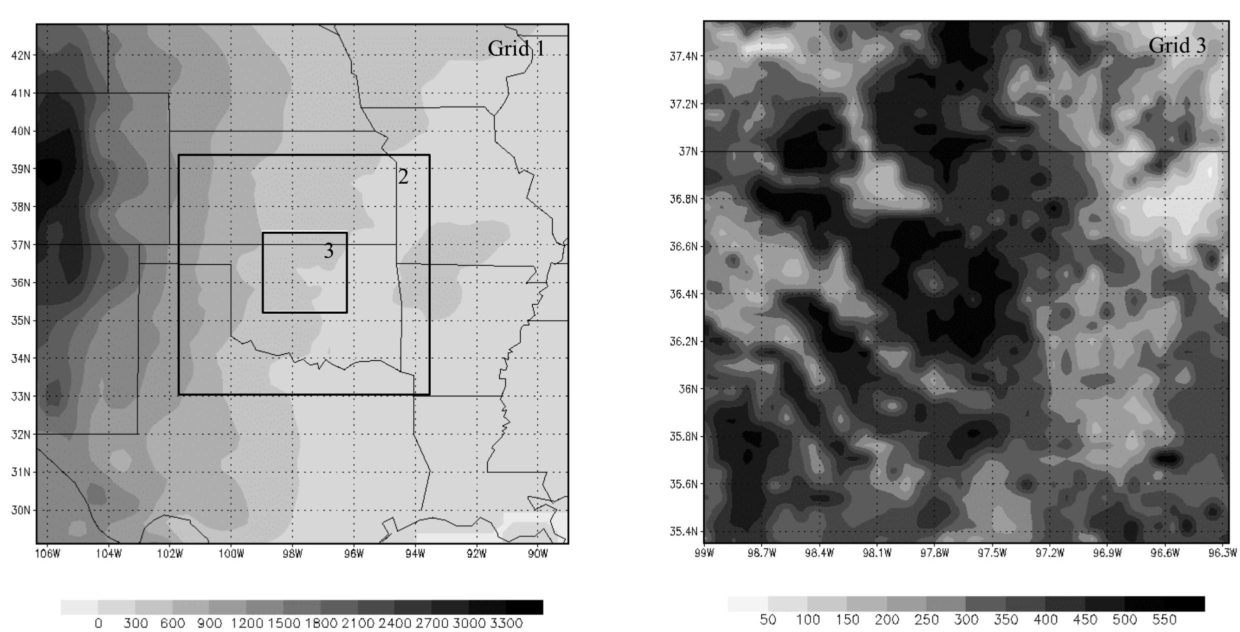

FIG. 1. (a) The full RAMS simulation domain (Grid 1) showing surface topographic height (m) and the locations of the nested Grids 2 and 3. (b) Grid 3 surface SH flux (W m^{-2}) at 1300 LST (1900 UTC) on 13 Jul 1995.

tial landscape, rather than day-to-day variations in meteorology, which plays a dominant role in the observed surface flux heterogeneity. While topography is often an additional and crucial forcing factor for PBL flow, the terrain of the ARM/CART site is relatively flat (Fig. 1a), and removing the influence of topography does not qualitatively affect our simulation results.

Each simulation covers 12 h, from 0600 to 1800 local standard time (LST; 1200 to 2400 UTC). We initialize each simulation using geopotential height, winds, temperature, and relative humidity from the National Centers for Environmental Prediction–National Center for Atmospheric Research (NCEP–NCAR) reanalysis project (Kalnay et al. 1996). The lateral boundary regions of Grid 1 are nudged during each model time step toward the reanalyses that are updated every 6 h.

To aid in the interpretation of the model results, we use 2-km resolution visible imagery from the Geostationary Operational Environmental Satellite (*GOES-8*) and composited rain gauge/WSR-88D radar rainfall measurements from the Arkansas-Red Basin River Forecast Center (ABRFC) collected as part of ESOP-95 (more information about these GCIP datasets can be found online at www.srh.noaa.gov/abrfc and www.ogp.noaa.gov/mpe/gcip/index.htm). The results we show here illustrate how model simulations, coupled with complementary observations, provide a powerful method for answering complex questions about the dynamics of land–atmosphere interactions at the mesoscale.

3. Results

a. Landscape-induced mesoscale circulations

Figures 2a,b show the simulated mid-PBL vertical velocity (w) field at two times, 1200 and 1530 LST

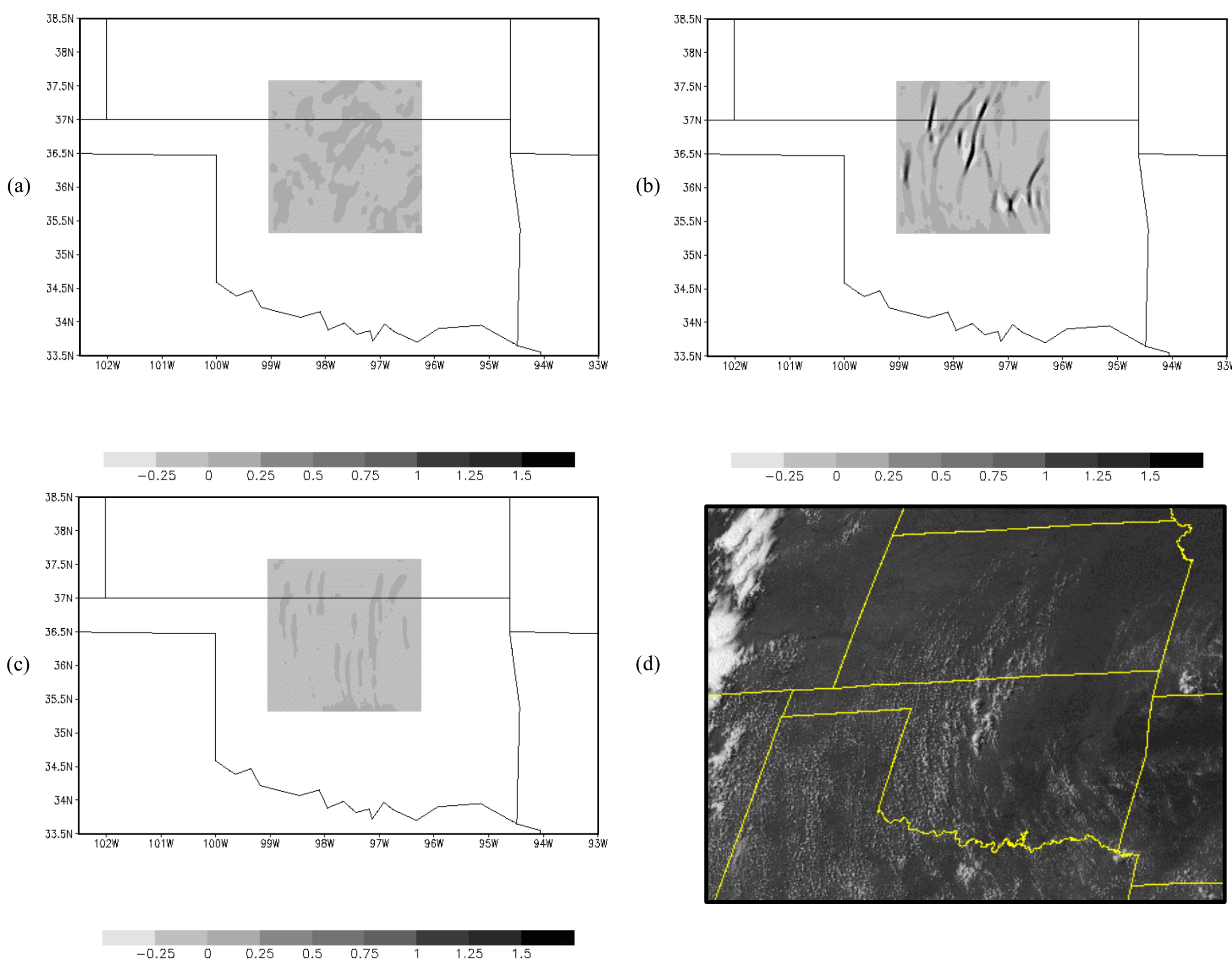

FIG. 2. All panels are for 13 Jul 1995. (a) RAMS simulated w (m s^{-1}) at 1117-m altitude at 1200 LST. (b) RAMS simulated w (m s^{-1}) at 1117-m altitude at 1530 LST. (c) RAMS simulated w (m s^{-1}) at 1117-m altitude at 1530 LST. For this simulation, the Grid 3 surface SH and LH fluxes were replaced by their domain-averaged values. (d) *GOES-8* satellite visible image at 1515 LST.

for the 13 July case. At 1200 LST (Fig. 2a), relatively weak upward motion of a few centimeters per second is located over patches of large SH flux (recall Fig. 1b) with scales on the order of a few tens of kilometers. Over the course of the afternoon, a series of coherent circulations with strong upward motion on the order of 1–2 m s^{-1} gradually evolve (Fig. 2b), as air flowing from high-LH (cooler) to high-SH (warmer) areas converge. Over some locations, this circulation penetrates from the surface to a height of more than 3 km.

To highlight the impact of the surface variability, rather than simply the mean surface conditions, we performed an additional simulation of the 13 July case, but with the realistic surface SH and LH fluxes replaced with their mean values over the Grid 3 domain, thus eliminating any mesoscale heterogeneity. The resulting SH and LH flux fields are not completely homogeneous, as we impose a random perturbation at each grid cell of amplitude 10 W m^{-2}, but the inhomogeneity that is present is small in amplitude and exists only at the 2-km horizontal scale of a single grid element. As seen in Fig. 2c, because the mesoscale surface heterogeneity has been eliminated, this mean flux case, rather than developing any organized circulation, has very weak vertical motion, probably resulting from gentle upslope flows, with peak *w* values of only about 0.05 m s^{-1} (compared to over 2 m s^{-1} in Fig. 2b). This contrast in atmospheric response between homogeneous and heterogeneous surfaces is in agreement with some previous theoretical studies, as noted above (Vidale et al. 1997; Baidya Roy and Avissar 2000; Avissar and Schmidt 1998; Dalu et al. 1996).

One important question is how to compare the model results with observations of clouds and precipitation. One shortcoming of the case study simulations described here is that, while RAMS was able to produce strong, coherent mesoscale circulations in response to the realistic meteorological and surface forcing, it produced very little cloudiness and precipitation: much less than the observed amounts for the days on which any clouds were reported. The failure of modeled convection and microphysics to produce realistic cloudiness is an important issue for mesoscale modeling in general, and a comprehensive investigation of why these simulations also failed to produce enough is beyond the scope of this study. Possible explanations might include insufficiently high horizontal resolution, given that we do not use any convective parameterization for Grid 3: while a 2-km grid spacing may be adequate for resolving some large cumulus, smaller clouds would be missed. In addition, this grid spacing might not provide vigorous enough updrafts to produce convective clouds in most areas where the model predicts rising motion. Higher resolution simulations can be used to address this issue, but the drawback is that they are extremely computationally expensive. Other factors could be related to characteristics of the RAMS microphysics package or inaccuracies in the data used to initialize and nudge the model. For example, if the model atmosphere is initially too dry, clouds might not form even in the presence of strong updrafts. Given these obstacles, our best option for providing observational validation of our simulated mesoscale circulations is therefore to compare the model-predicted *w* field which clearly shows the pattern of the circulations, and which is the best indicator of where we would expect to find clouds, with any observed clouds and rainfall. The key is to determine if the model is correctly reproducing the actual dynamics over the ARM/CART, and whether or not RAMS produces the correct cloudiness in response to these dynamics is a secondary concern at this stage.

That the simulated circulation pattern forced by the landscape heterogeneity is undoubtedly a real-world feature is demonstrated by the excellent correspondence between the simulated *w* field and the satellite cloud image (Fig. 2d), and composited rainfall measurements (Fig. 3). The clouds and precipitation are oriented along the linear, N–S convergence lines of strong upward motion. The model is able to capture not only a snapshot agreement, but correctly reproduces the evolution in time of the convergence field as diagnosed by successive hourly rainfall composites (Fig. 3); in the observations, the broadly V-shaped precipitation zone moves northward under the influence of the prevailing southerly wind and dissipates over the course of the late afternoon, and the model correctly captures this behavior.

The satellite observations indicate that two other of the remaining five case-study days (6, 21 July) also have clouds, and a comparison between the *w* fields and the satellite imagery for these days also shows good agreement between the location and orientation of the clouds and the simulated patterns of upward motion (Fig. 4). This agreement provides a high level of confidence in the ability of the model to correctly represent the essential physics of the organization of the atmospheric flow by the landscape pattern and therefore allows us to use the model results to illuminate details, over the full 65 000 km^2 Grid 3 domain, of the evolution, intensity, and transport properties of the circulations for which there are no suitable observations.

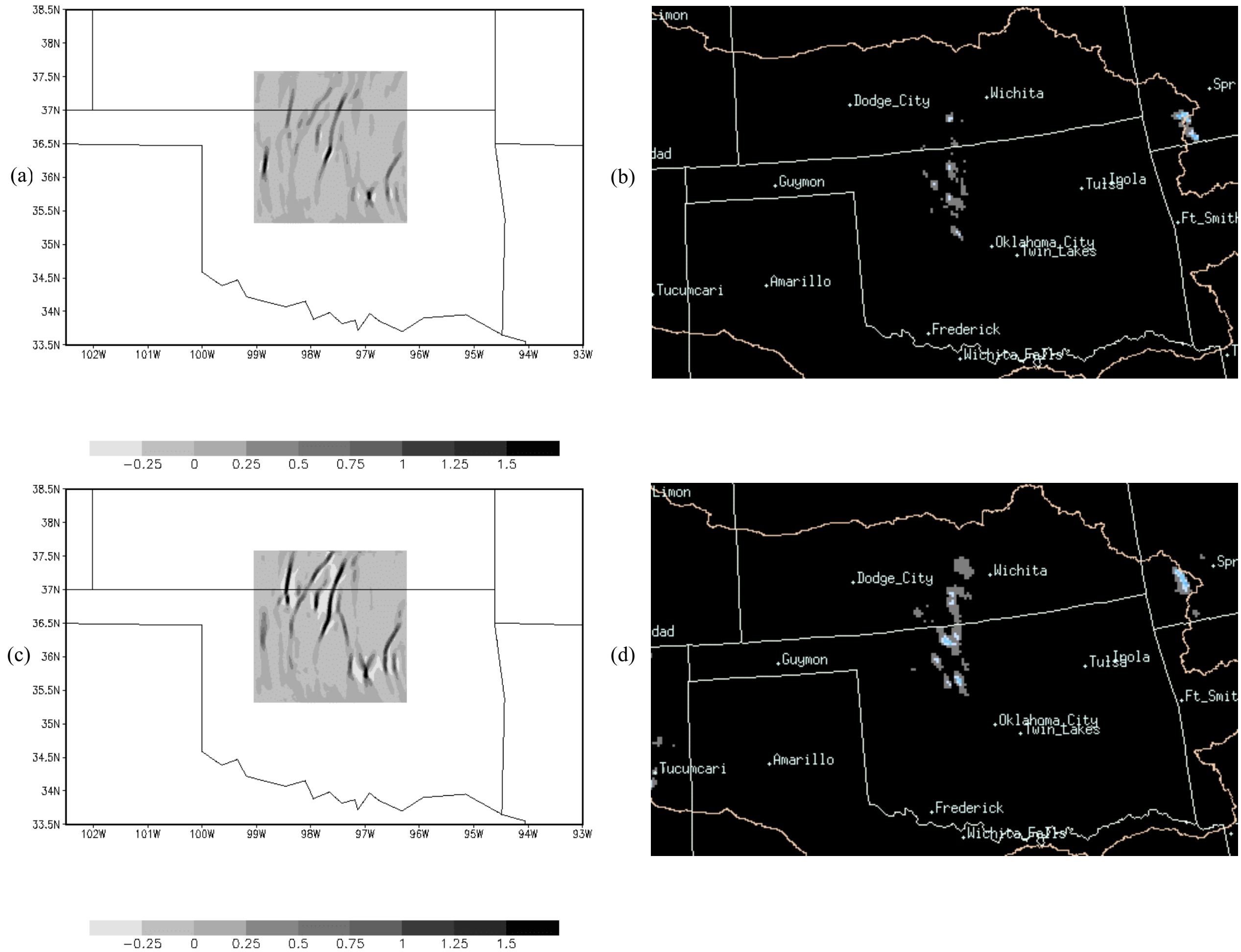

FIG. 3. (a)–(h) For 13 Jul 1995. (a) RAMS simulated w (m s^{-1}) at 1117-m altitude at 1500 LST. (b) ABRFC accumulated precipitation composite for 1500–1600 LST. (c) RAMS simulated w (m s^{-1}) at 1117-m altitude at 1600 LST. (d) ABRFC accumulated precipitation composite for 1600–1700 LST. Precipitation amounts are on the order of 0.1 in. h^{-1}.

That the cloud and w pattern is different among these three days, and that indeed there are no clouds on the remaining three (7, 10, 12 July; not shown), illustrates another fundamental point: a basically similar pattern of surface forcing can interact with different ambient meteorology to produce different atmospheric responses. Recalling Fig. 1b, it is clear that there are many different "choices" of surface flux patch patterns with, for example, an approximately 50-km patch scale. The induced circulations on each of the six days are comparably strong, as summarized in Table 1 (the peak w values are all large, on the order of 1 m s^{-1} or greater), and in each case they cover a large fraction of the domain and are properly classifiable as mesoscale. Nevertheless, they take on different orientations and peak locations in response to differences in large-scale meteorology.

Additionally, for a given circulation pattern and intensity, whether and how much cloud formation occurs depends strongly on the ambient moisture profile (Bougeault et al. 1991; Avissar and Liu 1996; Liu et al. 1999). The contrast between the 12 and 21 July cases is instructive. While the peak w value for 21 July is the lowest of any of the days (Table 1), and the value for 12 July much higher (i.e., the dynamical driving force for cloud formation is much stronger), convective clouds form on 21 and not 12 July simply because 12 July is a much drier day, and therefore even a very strong circulation is unable to produce clouds. It is important to keep this issue in mind when considering global impacts of land use changes on clouds and precipitation. For example, we point out that overall conditions are relatively dry over OK/KS in July compared to some other regions of the globe with substantial observed mesoscale surface heterogeneity

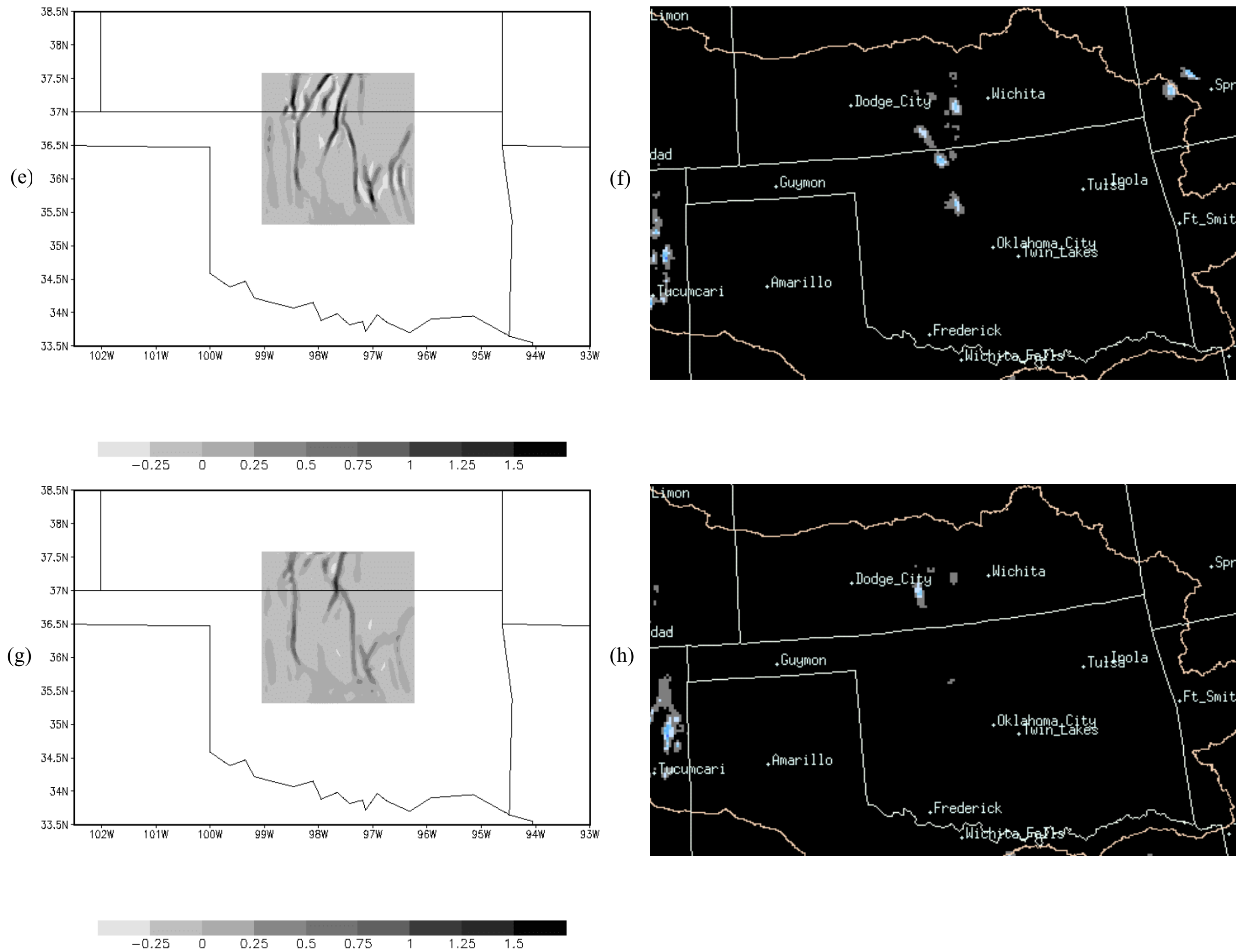

FIG. 3 (*continued*). (e) RAMS simulated w (m s^{-1}) at 1117-m altitude at 1700 LST. (f) ABRFC accumulated precipitation composite for 1700–1800 LST. (g) RAMS simulated w (m s^{-1}) at 1117-m altitude at 1800 LST. (h) ABRFC accumulated precipitation composite for 1800–1900 LST.

(e.g., Amazonia), and much stronger cloud and precipitation responses might be expected elsewhere given similar intensities of landscape–atmosphere effects.

b. Vertical fluxes

To demonstrate the important role these circulations play in transporting heat and moisture vertically, we calculated the three-dimensional SH and LH fluxes by both the resolved motions in the model, or mesoscale fluxes (i.e., vertical SH and LH fluxes due to motions with scales larger than the 2-km model grid spacing), and the subgrid-scale, parameterized turbulent fluxes (see Avissar and Chen 1993 for definitions and how to calculate the mesoscale fluxes). These mesoscale fluxes are one measure of the intensity of the landscape-induced circulations, and the peak domain-averaged mesoscale LH fluxes for each case day are summarized in Table 1.

Figure 5 shows mesoscale, turbulent, and total (mesoscale + turbulent) LH flux, averaged over the Grid 3 domain at 1600 LST (the peak mesoscale fluxes occur in the late afternoon, approximately three hours later than the peak surface SH flux), for both the mean surface flux and variable (realistic) surface flux 13 July simulations (recall Figs. 2b,c). We only show mesoscale LH flux because it tends to be larger than SH flux for the cases considered here. The key result is that mesoscale landscape heterogeneity significantly alters the magnitude and shape of the vertical flux profile for given large-scale-averaged surface fluxes and given meteorological conditions. Shifting some of the vertical transport from small (turbulent) scales to larger (mesoscale) scales produces substantially more total LH transport (on the order of 150 W m^{-2} in Fig. 5d) in the upper PBL, with correspondingly significant implications for production of clouds and precipitation

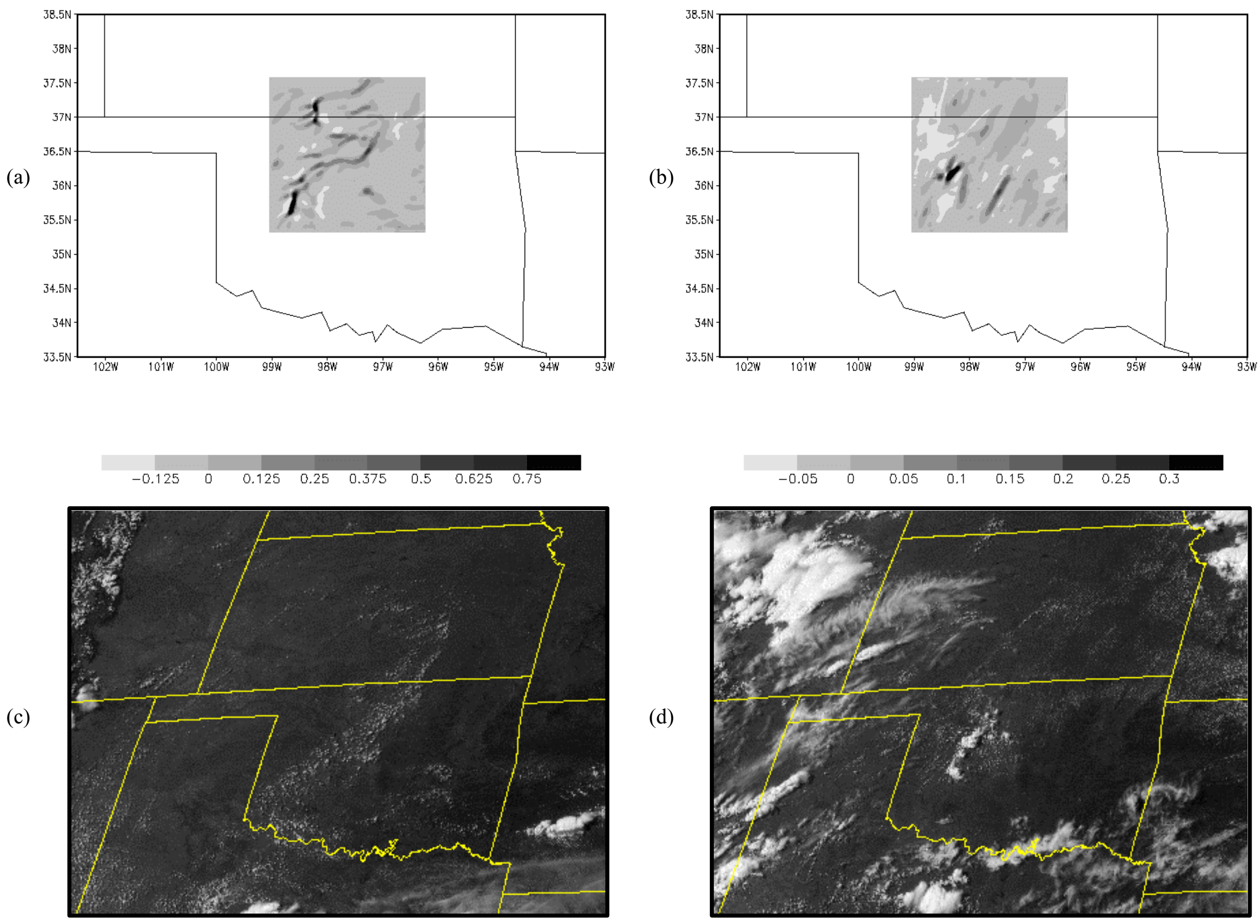

FIG. 4. (a) RAMS simulated w (m s^{-1}) at 1117-m altitude at 1530 LST on 6 Jul 1995. (b) RAMS simulated w (m s^{-1}) at 1117-m altitude at 1530 LST 21 Jul 1995. (c) *GOES-8* satellite visible image at 1515 LST on 6 Jul 1995. (d) *GOES-8* satellite visible image at 1515 LST on 21 Jul 1995.

TABLE 1. For each of the six case-study simulations, shown are maximum, updraft velocity (w) for the given day and maximum domain-averaged vertical mesoscale LH flux. The domain averages are over the entire Grid 3 horizontal area. For all cases, the maximum w and mesoscale LH flux occurred in the mid- to upper PBL during the late afternoon.

Case	Max w (m s^{-1})	Max domain-mean mesoscale LH flux (W m^{-2})
6 Jul	3.36	127.6
7 Jul	3.03	159.0
10 Jul	2.31	120.2
12 Jul	3.11	69.5
13 Jul	4.47	174.4
21 Jul	1.38	50.5

as well as for the energy available to drive the overall atmospheric circulation. The physical explanation for this process is that the mesoscale circulations result in enhanced *vertical* moisture transport because of their ability to transport moisture *horizontally*, from areas where surface LH flux is large, but the PBL is consequently shallow, to areas where surface LH flux is small but surface SH flux is large, and where therefore the PBL is deep and the moisture can penetrate higher. As a result, over the portions of the domain with strong mesoscale updrafts, the mesoscale fluxes in the mid- and upper PBL are much larger than the turbulent fluxes (often reaching into the thousands of Watts per square meter), and this is reflected in the domain averages. The second, more subtle, factor is that, in addition to this direct transport by the mesoscale circulation, the changes in airmass movement resulting from the mesoscale flow additionally change the turbulent transport (see also Vidale et al. 1997), as illustrated in Fig. 5b by the larger values of turbulent LH flux above 1700 m for the heterogeneous surface case. All scales of motion are therefore influenced by the surface heterogeneity.

c. The impact of the background wind

Some model and analytical studies have indicated that, except under very weak large-scale background wind conditions (e.g., on the order of 2–3 m s^{-1} or less), landscape-induced mesoscale flows are inhibited, and the corresponding mesoscale fluxes are therefore also very weak (Avissar and Schmidt 1998; Wang et al. 1996; Liu et al. 1999); hence the most common argument against their climatological importance, that is, the percentage of time these landscape heterogeneity effects are significant is expected to be small (Zhong and Doran 1997, 1998). This view has been challenged recently (Vidale et al. 1997; Wang et al. 1998), and our results demonstrate for a range of cases that increasing large-scale wind does not necessarily inhibit these mesoscale circulations.

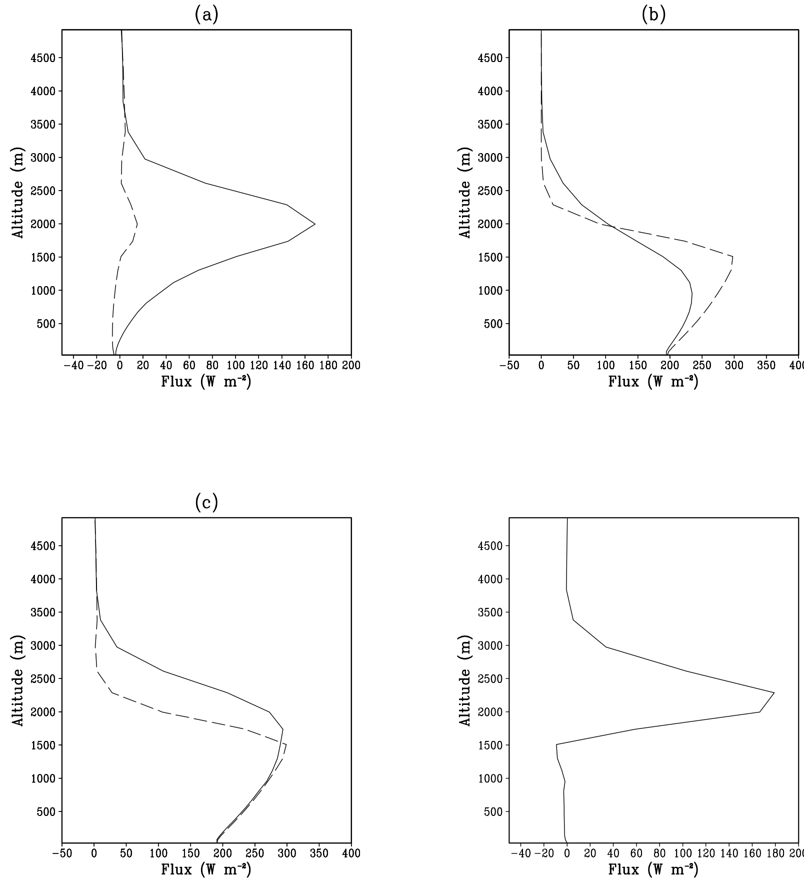

FIG. 5. (a) Grid 3 averaged mesoscale LH flux (W m^{-2}) at 1600 on 13 Jul 1995. The solid curve is for the realistic surface flux run, and the dashed curve is for the mean surface flux run. (b) Same as (a) but for Grid 3 averaged turbulent LH flux. (c) Same as (a) but for Grid 3 averaged total (mesoscale + turbulent) LH flux. (d) The difference in total LH flux between the runs with mean and realistic surface flux.

Figure 6 shows vertical–longitude cross sections of simulated *u* and *v* at 0800, 1200, and 1600 LST along 36.8°N latitude (just south of the Oklahoma–Kansas border) for the 13 July case. This figure illustrates two major points. First, the wind velocities are not particularly small, approaching 10 m s^{-1} or greater in the upper portions of the PBL at various points during the day. Second, one can clearly see the evolution of the mesoscale circulations by 1600 LST, visible here primarily as zonal, near-surface convergence and upper-PBL divergence cells (Fig. 6e), and one can also clearly see that this evolution is essentially decoupled from the evolution of the large-scale background flow in the free troposphere. This behavior is typical for all the other days studied, all with essentially comparable mean winds (Fig. 7), and we find no particular relationship between overall synoptic-scale wind speed and the viability or intensity of the landscape-forced mesoscale circulations. Indeed, 7 July, the day with the highest mean winds in the lowest part of the atmosphere (Fig. 7) also has one of the highest mean mesoscale LH fluxes (Table 1). One reason that strong circulations resulting from mesoscale horizontal gradients probably occur more frequently than suspected by some investigators could be that, with a realistic two-dimensional horizontal wind field and two-dimensional surface heterogeneity, the large-scale wind will often blow perpendicular to the surface gradient at some locations, and parallel to it at others. For the case shown in Fig. 6, the strongest winds are N–S, whereas the mesoscale circulation cells are primarily oriented E–W. Previous numerical studies often considered the impact of a unidirectional background wind always blowing parallel to the surface flux gradient (e.g., see Liu et al. 1999, among many others). In addition, winds parallel to the thermal gradient, rather than always smoothing it out, can sometimes squeeze the isotherms closer together, thus intensifying the pressure contrasts across the landscape discontinuity and producing stronger mesoscale circulations (Pielke 1984).

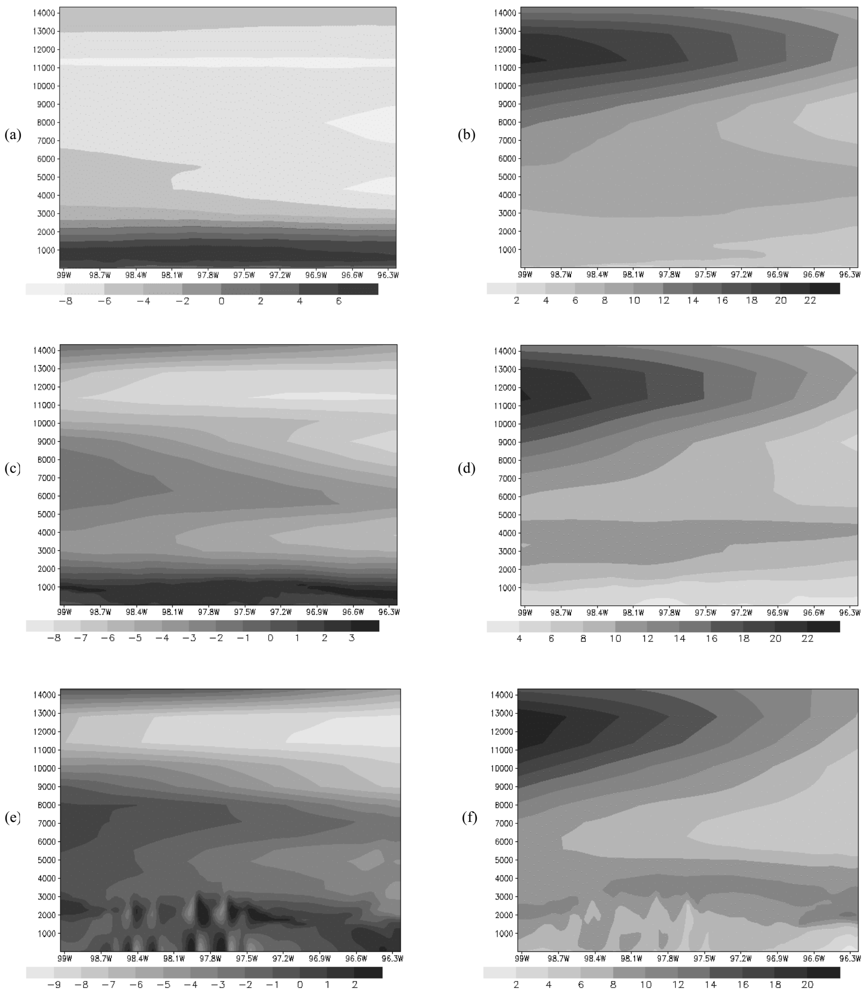

FIG. 6. (a)–(f) For 13 Jul 1995. (a) Altitude–longitude cross section of RAMS simulated u (m s^{-1}) at 0800 LST. (b) Altitude–longitude cross section of RAMS simulated v (m s^{-1}) at 0800 LST. (c) Same as (a) but for 1200 LST. (d) Same as (b) but for 1200 LST. (e) Same as (a) but for 1600 LST. (f) Same as (b) but for 1600 LST.

Instead of having an inhibiting effect, the synoptic-scale wind plays a key role in orienting, steering, and advecting the landscape-induced mesoscale circulations. The differences in mesoscale circulation patterns among the different case days, and the northward movement of the precipitation system on 13 July by the large-scale southerly wind (recall Fig. 3), result from this interaction between the mesoscale and the synoptic-scale. This finding has important implications for our understanding of the wider area and longer time impacts of landscape heterogeneity on the atmosphere. First, since these mesoscale effects can occur under conditions of moderate and strong synoptic-scale winds, they probably are important more often (climatologically) than previously assumed. Second, the advection of mesoscale cloud and precipitation systems away from the local area whose surface conditions generated the circulation complicates the problem of determining radiative and hydrological feedbacks between the land surface and the atmosphere.

4. Conclusions

The results shown here demonstrate that, by changing the scale and properties of the naturally occurring land surface elements, human influences can significantly affect local weather and climate, at least in the short term. Since both natural and human-modified heterogeneous landscapes are ubiquitous around the globe (e.g., snow/soil, land/water, pasture/forest, city/country), such atmospheric effects must influence global climate today. However, the extent of this influence, and the longer-term impacts of accelerating land use changes on future regional and global climate, are currently unknown. At present, our only tools for climate prediction are GCMs, and the efficacy of such models for adequate risk assessment depends most importantly on how well they simulate the various climate processes, rather than any particular climate state. A good representation of present-day climate is worthless from a prediction standpoint without confidence in the model's ability to realistically simulate components of the climate system, such as the land surface, that can evolve slowly and interact nonlinearly with the atmosphere over long timescales. Since most GCMs used for climate prediction can only explicitly resolve scales of hundreds of kilometers, one of the key aspects of this ongoing drive for improvement lies in finding appropriate parameterizations of processes that occur at scales smaller than this. For heterogeneous land surfaces, both the underlying heterogeneity and the atmospheric response, in the form of turbulent and mesoscale motions, are subgrid-scale processes in GCMs, and their effects, if significant,

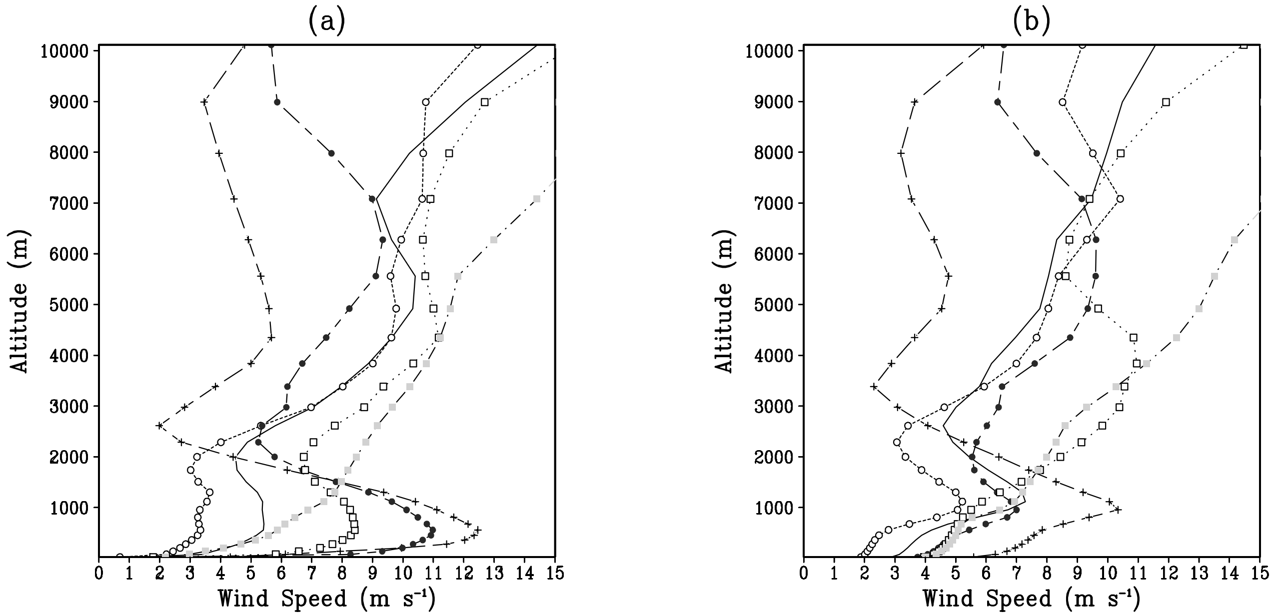

FIG. 7. (a) Grid 3 averaged wind speed (m s^{-1}) at 0800 LST for each of the six case-study days. (b) Grid 3 averaged wind speed (m s^{-1}) at 1200 LST for each of the six case-study days. (6 July: solid line; 7 July: long dashed line with cross symbols; 10 July: short dashed line with open circles; 12 July: long–short dashed line with closed circles; 13 July: dotted line with open squares; 21 July: dashed–dotted line with closed squares.) We show early morning and noon wind here because they are illustrative of the large-scale wind conditions existing prior to the full development of any landscape-generated mesoscale circulations. The winds later in the day include the effects of these circulations, and thus cannot properly be considered to reflect the ambient synoptic-scale environment in which such circulations must form.

must be accounted for. While current GCMs employ parameterizations for subgrid-scale flow, these parameterizations are based solely on observations and theories of turbulence processes over homogeneous landscapes, and consequently, important mesoscale effects like the ones described in this study are completely ignored. Thus, we are unable to correctly account for the effects of landscape heterogeneity in our simulations of present climate, and we are ill equipped to predict the full consequences of future land use changes. To address this, a few preliminary GCM parameterizations of mesoscale fluxes have already been proposed (Liu et al. 1999; Avissar and Chen 1993; Arola 1999; Zeng and Pielke 1995; Lynn et al. 1995a), and the results shown here should stimulate further efforts to implement realistic representations of these processes in state-of-the-art climate models with the aim of addressing current problems in, for example, simulating continental shallow convection (Berbery et al. 1999), correctly representing albedo and hydrological feedbacks between the surface and the atmosphere (Betts et al. 1996), and improving simulations of future climate change.

Acknowledgments. This research was supported by the National Oceanic and Atmospheric Administration under Grant NA86GP0514. The views expressed herein are those of the authors and do not necessarily reflect the views of this agency. Thanks to J. C. Doran and S. Zhong of the Department of Energy's Pacific Northwest National Laboratory for graciously making their surface flux data available to us. Thanks also to S. Baidya Roy for useful discussions. We obtained the NCEP–NCAR reanalysis data from NCAR, which is funded by the National Science Foundation.

References

Arola, A., 1999: Parameterization of turbulent and mesoscale fluxes for heterogeneous surfaces. *J. Atmos. Sci.,* **56,** 584–598.

Avissar, R., and R. A. Pielke, 1989: A parameterization of heterogeneous land-surface for atmospheric numerical models and its impact on regional meteorology. *Mon. Wea. Rev.,* **117,** 2113–2136.

——, and F. Chen, 1993: Development and analysis of prognostic equations for mesoscale kinetic energy and mesoscale (subgrid scale) fluxes for large-scale atmospheric models. *J. Atmos. Sci.,* **50,** 3751–3774.

——, and Y. Liu, 1996: Three-dimensional numerical study of shallow convective clouds and precipitation induced by land-surface forcing. *J. Geophys. Res.,* **101,** 7499–7518.

——, and T. Schmidt, 1998: An evaluation of the scale at which ground-surface heat flux patchiness affects the convective boundary layer using large-eddy simulations. *J. Atmos. Sci.,* **55,** 2666–2689.

Baidya Roy, S., and R. Avissar, 2000: Scales of response of the convective boundary layer to surface heterogeneity. *Geophys. Res. Lett.,* **27,** 533–536.

Betts, A. K., J. H. Ball, A. C. M. Beljaars, M. J. Miller, and P. A. Viterbo, 1996: The land surface–atmosphere interaction: A review based on observational and global modeling perspectives. *J. Geophys. Res.,* **101,** 7209–7225.

Bougeault, P., B. Bret, P. Lacarrere, and J. Noilhan, 1991: An experiment with an advanced surface parameterization in a mesobeta-scale model. Part II: The 16 June 1986 simulation. *Mon. Wea. Rev.,* **119,** 2374–2392.

Brown, M. E., and D. L. Arnold, 1998: Land-surface-atmosphere interactions associated with deep convection in Illinois. *Int. J. Climatol.,* **18,** 1637–1653.

Chen, F., and R. Avissar, 1994a: The impact of land-surface wetness heterogeneity on mesoscale heat fluxes. *J. Appl. Meteor.,* **33,** 1323–1340.

——, and ——, 1994b: Impact of land-surface moisture variability on local shallow convective cumulus and precipitation in large-scale models. *J. Appl. Meteor.,* **33,** 1382–1401.

Coughlan, M., and R. Avissar, 1996: The Global Energy and Water Cycle Experiment (GEWEX) Continental-Scale International Project (GCIP): An overview. *J. Geophys. Res.,* **101,** 7139–7147.

Cutrim, E., D. W. Martin, and R. Rabin, 1995: Enhancement of cumulus clouds over deforested lands in Amazonia. *Bull. Amer. Meteor. Soc.,* **76,** 1801–1805.

Dalu, G. A., R. A. Pielke, M. Baldi, and X. Zeng, 1996: Heat and momentum fluxes induced by thermawql inhomogeneities. *J. Atmos. Sci.,* **53,** 3286–3302.

Doran, J. C., W. J. Shaw, and J. M. Hubbe, 1995: Boundary layer characteristics over areas of inhomogeneous surface fluxes. *J. Appl. Meteor.,* **34,** 559–571.

——, J. M. Hubbe, J. C. Liljegren, W. J. Shaw, G. J. Collatz, D. R. Cook, and R. L. Hart, 1998: A technique for determining the spatial and temporal distribution of surface fluxes of heat and moisture over the southern Great Plains cloud and radiation testbed. *J. Geophys. Res.,* **103,** 6109–6121.

Hubbe, J. M., J. C. Doran, J. C. Liljegren, and W. J. Shaw, 1997: Observations of spatial variations of boundary layer structure over the southern Great Plains cloud and radiation testbed. *J. Appl. Meteor.,* **36,** 1221–1231.

Kalnay, E., and Coauthors, 1996: The NCEP/NCAR 40-Year Reanalysis Project. *Bull. Amer. Meteor. Soc.,* **77,** 437–471.

Liston, G. E., and R. A. Pielke, 2000: A climate version of the Regional Atmospheric Modeling System. *Theor. Appl. Climatol.,* **66,** 29–47.

Liu, Y., C. P. Weaver, and R. Avissar, 1999: Toward a parameterization of mesoscale fluxes and moist convection induced by landscape heterogeneity. *J. Geophys. Res.,* **104,** 19 515–19 533.

Lynn, B. H., F. Abramopoulos, and R. Avissar, 1995a: Using similarity theory to parameterize mesoscale heat fluxes generated by subgrid-scale landscape discontinuities in GCMs. *J. Climate,* **8,** 932–951.

——, D. Rind, and R. Avissar, 1995b: The importance of mesoscale circulations generated by subgrid-scale landscape heterogeneities in general circulation models. *J. Climate,* **8,** 191–205.

Mahfouf, J.-F., E. Richard, and P. Mascart, 1987: The influence of soil and vegetation on the development of mesoscale circulation. *J. Climate Appl. Meteor.,* **26,** 1483–1495.

Mahrt, L., J. Sun, D. Vickers, J. I. MacPherson, J. R. Pederson, and R. Desjardins, 1994: Observations of fluxes and inland breezes over a heterogeneous surface. *J. Atmos. Sci.,* **51,** 2484–2499.

Ookouchi, Y., M. Segal, R. C. Kessler, and R. A. Pielke, 1984: Evaluation of soil moisture effects on generation and modification of mesoscale circulations. *Mon. Wea. Rev.,* **112,** 2281–2292.

Pielke, R. A., 1984: *Mesoscale Meteorological Modeling.* Academic Press, 612 pp.

——, G. Dalu, J. S. Snook, T. J. Lee, and T. G. F. Kittel, 1991: Nonlinear influence of mesoscale land use on weather and climate. *J. Climate,* **4,** 1053–1069.

——, and Coauthors, 1992: A comprehensive meteorological modeling system—RAMS. *Meteor. Atmos. Phys.,* **49,** 69–91.

Pinty, J.-P., P. Mascart, E. Richard, and R. Rosset, 1989: An investigation of mesoscale flows induced by vegetation inhomogeneities using an evapotranspiration model calibrated against HAPEX-MOBILHY data. *J. Appl. Meteor.,* **28,** 976–992.

Rabin, R. M., S. Stadler, P. J. Wetzel, D. J. Stensrud, and M. Gregory, 1990: Observed effects of landscape variability on convective clouds. *Bull. Amer. Meteor. Soc.,* **71,** 272–280.

Segal, M., R. Avissar, M. C. McCumber, and R. A. Pielke, 1988: Evaluation of vegetation effects on the generation and modification of mesoscale circulations. *J. Atmos. Sci.,* **45,** 2268–2292.

——, W. E. Schreiber, G. Kallos, J. R. Garratt, A. Rodi, J. Weaver, and R. A. Pielke, 1989: The impact of crop areas in northeast Colorado on midsummer mesoscale thermal circulations. *Mon. Wea. Rev.,* **117,** 809–825.

Sellers, P. J., and Coauthors, 1996: A revised land surface parameterization (SiB2) for atmospheric GCMs. Part I: Model formulation. *J. Climate,* **9,** 676–705.

Seth, A., and F. Giorgi, 1996: Three-dimensional model study of organized mesoscale circulations induced by vegetation. *J. Geophys. Res.,* **101,** 7371–7391.

Stokes, G. M., and S. E. Schwartz, 1994: The Atmospheric Radiation Measurement (ARM) program: Programmatic background and design of the cloud and radiation test bed. *Bull. Amer. Meteor. Soc.,* **75,** 1201–1220.

Stull, R., 1988: *Boundary Layer Meteorology.* Kluwer Academic, 666 pp.

Vidale, P. L., R. A. Pielke, L. T. Steyaert, and A. Barr, 1997: Case study modeling of turbulent and mesoscale fluxes over the BOREAS region. *J. Geophys. Res.,* **102,** 29 167–29 188.

Wang, J., R. Bras, and E. A. B. Eltahir, 1996: A stochastic linear theory of mesoscale circulation induced by the thermal hetereogeneity of the land surface. *J. Atmos. Sci.,* **53,** 3349–3366.

——, E. A. B. Eltahir, and R. L. Bras, 1998: Numerical simulation of nonlinear mesoscale circulations induced by the thermal hetereogeneities of land surface. *J. Atmos. Sci.,* **55,** 447–464.

Yan, H., and R. A. Anthes, 1988: The effect of variations in the surface moisture on mesoscale circulations. *Mon. Wea. Rev.,* **116,** 192–208.

Zeng, X., and R. A. Pielke, 1995: Landscape-induced atmospheric flow and its parameterization in large-scale numerical models. *J. Climate,* **8,** 1156–1177.

Zhong, S., and J. C. Doran, 1997: A study of the effects of spatially varying fluxes on cloud formation and boundary layer properties using data from the southern Great Plains cloud and radiation testbed. *J. Climate,* **10,** 327–341.

——, and ——, 1998: An evaluation of the importance of surface flux variability on GCM-scale boundary-layer characteristics using realistic meteorological and surface forcing. *J. Climate,* **11,** 2774–2788.

With the development of meteorological science and the continual refinement of the technologies used in its practical application, the need to produce a new edition of the *International Meteorological Vocabulary* (IMV) became evident (the original edition was published in 1966). This volume is made up of a multilingual list of over 3500 terms arranged in English alphabetical order, accompanied by definitions in each of the languages (English, French, Russian, and Spanish) and an index for each language. This new edition has been augmented with numerous concepts relating to new meteorological knowledge, techniques, and concerns. It should help to standardize the terminology used in this field, facilitate communication between specialists speaking different languages, and aid translators in their work.

WMO No. 182, 784 pp., softbound, color-coded index, $95 (including postage and handling). Please send prepaid orders to: WMO Publications Center, American Meteorological Society, 45 Beacon St., Boston, MA 02108-3693. (Orders from U.S. and Canada only.)

World Meteorological Organization

International Meteorological Vocabulary

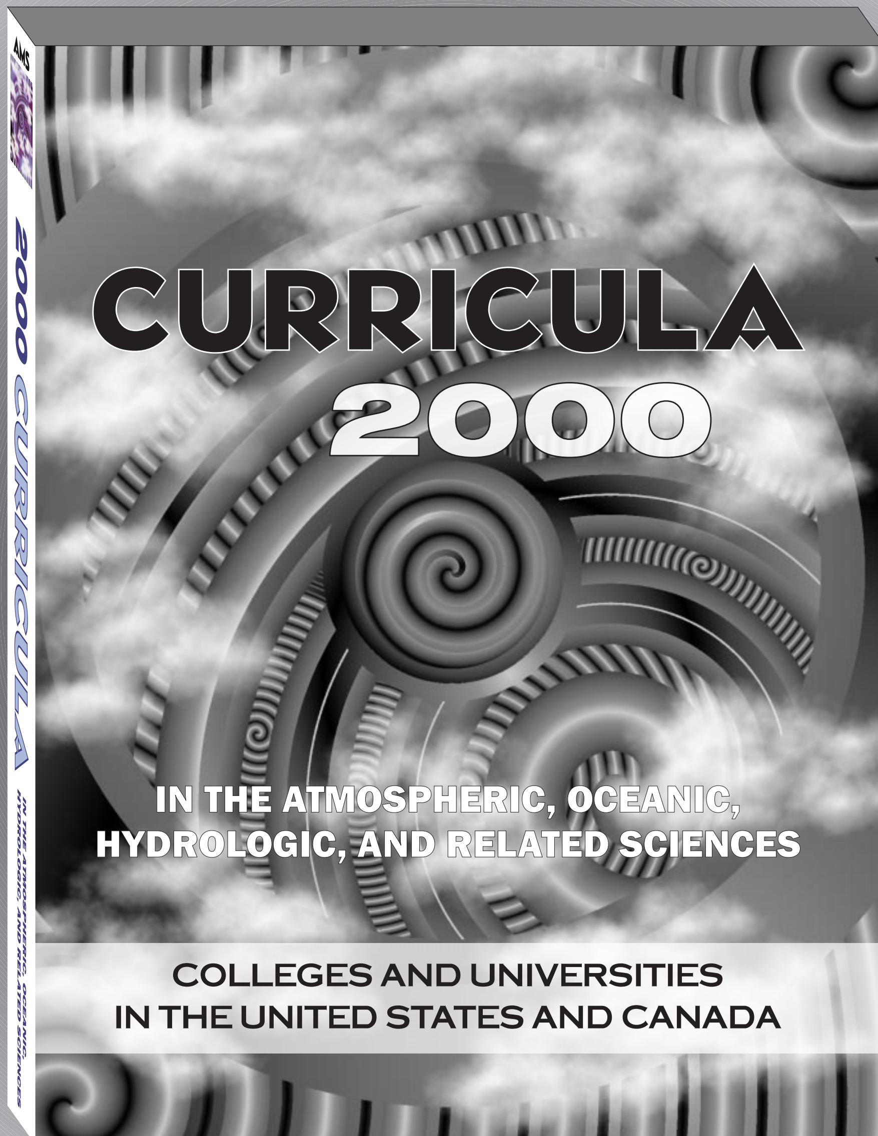

UPDATED 2000 EDITION!

The newly updated *Curricula* provides useful and detailed information on programs in the atmospheric sciences and closely related oceanic, hydrologic, and other sciences including undergraduate and graduate courses and degrees offered, types of financial support available, titles and amounts of research grants and contracts in effect, and background information and special interests of faculty members at universities in the United States and Canada.

The *Curricula* is available for $40/list, $30/AMS members and students, by sending prepaid orders to: **Order Department, AMS, 45 Beacon Street, Boston, MA 02108-3693**; call **617-227-2425** to order by phone using Visa, Mastercard, or American Express; or send e-mail to **amsorder@ametsoc.org.** Please make checks payable to the **American Meteorological Society.** The online version of the *Curricula* may be accessed free of charge from our Web site at www.ametsoc.org/AMS.

A JOINT PUBLICATION OF THE AMERICAN METEOROLOGICAL SOCIETY AND THE UNIVERSITY CORPORATION FOR ATMOSPHERIC RESEARCH